Sensors & Transducers Journal, Vol. 137, Issue 2, February 2012, pp. 74-84

www.sensorsportal.com

Sensors & Transducers

ISSN 1726-5479

http://www.sensorsportal.com

Studies on Gas Sensing Performance of $(Sn_{0.2}Ti_{0.8})O_2$ Thick Film Resistor

[1] P. D. HIRE, [1] V. B. GAIKWAD, [2] N. U. PATIL, [1] R. M. CHAUDHARI, [1] R. L. PATIL, [*3] G. H. JAIN

[1] Material Science Lab., K.T.H.M. College. Nashik - 422 002, India
[2] Dept of Physics, Arts, Science and Commerce College, Igatpuri - 422 303, India
[3] Dept of Physics, Arts, Science and Commerce College, Nandgaon - 423 106, India
E-mail: * gotanjain@rediffmail.com and [1] pdhdesrane@gmail.com

Received: 7 November 2011 /Accepted: 14 February 2012 /Published: 28 February 2012

Abstract: In this work we report the synthesis, microstructure, electric properties and sensing performance of $(Sn_{0.2}Ti_{0.8})\ O_2$ (ST) powder, were prepared by wet chemical method. Thick films were prepared by screen-printing technology. Structural and electrical analyses were performed and the results have been correlated. The pure ST film shows good response (S=12.6) to Cl_2 at 350 ^{0}C for gas concentration 400 ppm and CuO-modified ST film improves the selectivity and sensitivity and maximum response (S=50.2) was found to H_2S gas at 400 ^{0}C for same gas concentration. The characterization of the films was done by XRD, SEM and TGA. Crystallite size, surface area, Electric properties and gas sensitivity of the films were measured and presented. *Copyright © 2012 IFSA.*

Keywords: $(Sn_{0.2}Ti_{0.8})\ O_2$ (ST); Thick films; H_2S gas sensor; Sensitivity; Selectivity.

1. Introduction

The principle of operation of the most frequently used chemical sensors for hazardous gases such as CO, Cl_2 and H_2S involves a change in the surface resistance of the n-type metal oxide upon exposure to a specific gas. As far as the active element of the device is concerned, SnO_2 has by far surpassed other metal oxides, mainly due to its high sensitivity to the reducing atmosphere [1–4]. However, generally recognized poor selectivity and low thermodynamic stability of SnO_2 at elevated temperatures have given rise to the search for new active materials. The renewed interest in TiO_2 as a sensing medium stems from its remarkable resistance to reduction [6]. Mixed oxide compounds, such

as isostructural solid solutions of SnO_2–TiO_2, seem to be promising candidates for gas detection [7]. Complex oxide systems may benefit from the combination of the best sensing properties of their pure components. Despite numerous studies [8, 9] of the crystallographic structure and thermodynamic properties of SnO_2–TiO_2, the present knowledge of the material parameters seems to be rather limited.

Among the metal oxides, tin dioxide and titanium dioxide, due to their chemical and electrical properties, are particularly appealing both for basic research and for a wide variety of possible applications [10, 11]. Tin dioxide is the most common material in gas sensing, but it is widely used as transparent conductor and in heterogeneous catalysis; titanium dioxide is used as a photocatalyst, in solar cells, as an optical coating, in gas sensing, etc. Tin dioxide and titanium dioxide are both wide-gap semiconductors, showing several similarities in structural as well as in electronic properties. However, they exhibit also some peculiar differences, such as electrical conductivity and gas sensing behavior. The gas sensing mechanism in all polycrystalline n-type semiconductors is generally ascribed to the Schottky barrier formation at gas-semiconductor interface, leading to a negative surface charge accumulation, typically O− ions. The variation of the height of the intergranular barrier is the result of surface chemical reactions with environmental gases leading to electrical conductance modifications. The two materials differ in gas sensing behavior, being TiO_2 much less reactive versus reducing agents than SnO_2; however the mechanism of sensing seems to be common. The operation temperature of the two materials is very similar, in the range of 400–600 ^{0}C, which are typical of surface interaction mechanism, and not bulk one. Usually, mixed metal oxides and solid solutions have been considered for the superior performances shown in comparison to the single oxides [12-16]. In this context, we attempted to join advantages of the better characteristics of both materials: high gas sensitivity for SnO_2 and lower influence by humidity for TiO_2, and to overcome their disadvantages: poor selectivity for SnO_2 and high resistivity and the polymorphic transition with temperature accompanied by exaggerated grain growth for TiO_2 [17].

The goal of this paper is the synthesis of $(Sn_xTi_{1-x})O_2$ (ST) materials for x=0.2. More specifically, we aim at better information on: (i) the effectiveness of wet chemical method for preparing powders with controlled stoichiometry, x= 0.2 (ii) electronic properties and their changes in contact with reducing gases. Scanning Electron microscopy (SEM), X-ray diffraction (XRD) and specific surface area measurements were adopted to analyze the morphology, the crystalline structure and the mean grain radius. Finally, electrical measurements (electrical properties and gas sensing properties) have been performed.

2. Experimental

2.1. Powder Preparation

$(Sn_xTi_{1-x})O_2$ (x=0.2) solid-solution was obtained via wet chemical method starting from the stoichiometric solution of Pure (99.9 %) AR grade $SnCl_2 \cdot 2H_2O$ and $TiCl_3$. $(Sn_{0.2}Ti_{0.8})O_2$ solution ([Sn]:[Ti]=1:4) was synthesized by adding drop by drop $TiCl_3$ into solution of $SnCl_2$ mixed with water. For stoichiometry, the whole process was carried out by maintaining the solution under soft stirring at the temperature of 50 ^{0}C. The resulting colloids were sintered at 1000 ^{0}C for 10 h. Then this powder ground in an agate pastle–mortor to ensure sufficiently fine particle size [18, 19].

2.2. Paste and Thick Film Preparation

The thixotropic paste was formulated by mixing the resulting ST fine powder with a temporary binder as a mixture of organic solvents. The ratio of the inorganic to organic part was kept at 75:25 in formulating the paste.

The thixotropic paste was then used to prepare thick films. The paste was screening printed [20-22] on a glass substrate in a desired pattern (1.5 cm x 0.5 cm). The films were fired at 550 ^{0}C for 30 min. in air atmosphere to remove the residual.

2.3. Gas Sensing System

The sensing performance of the sensors was examined using a 'static gas sensing system' [23]. A D.C. constant voltage was applied across the film using two electrodes and current was measured by using digital picoammeter. To heat the sample up to required operating temperatures the heater was fixed on the base plate. A thermocouple was connected to a digital temperature indicator. A gas inlet valve was fitted at one of the ports of the base plate. The required gas concentration inside the static system was achieved by injecting a known volume of test gas using a gas-injecting syringe. Air was allowed to pass into the glass dome after every gas exposure cycle.

3. Materials Characterization

3.1. X-ray Diffractogram

Fig. 1 depicts an XRD pattern of ST powder. X-ray diffraction analysis of this powder was carried out in the 20-80 deg (2θ) range using Cu-Kα (with λ= 1.54Å, 40 kV, 30 mA) radiation. The observed peaks match well with the reported ASTM data confirming the polycrystalline tetragonal pervoskite phases. The higher peak intensities of an XRD pattern are due to the better crystallinity. We can observe that the sample included rutile TiO_2 phase and casseterrite SnO_2 phase. Smaller intensity of SnO_2 peaks due to less percentage of it in (Sn, Ti) O_2 powder.

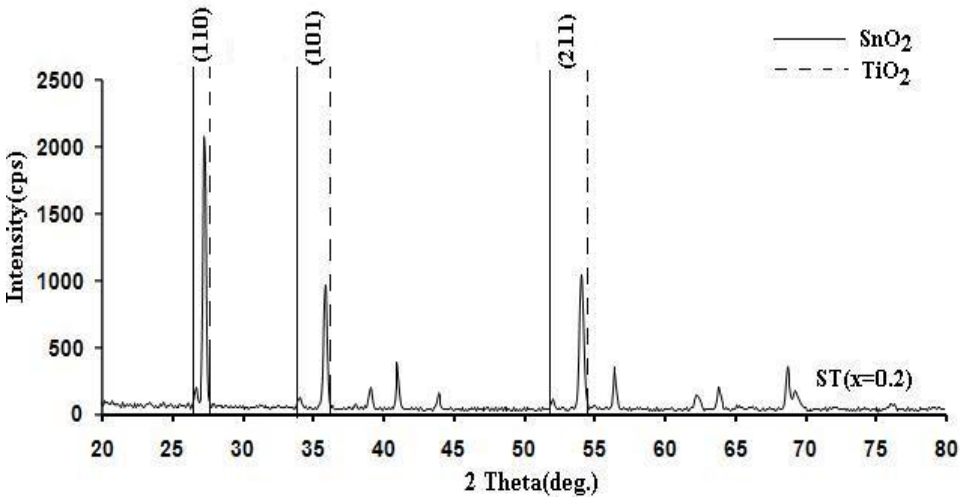

Fig. 1. XRD pattern of pure ST powder; (1 1 0), (1 0 1) and (2 1 1) Bragg reflections are compared with the positions of the same peaks related to pure SnO_2 (solid line) and pure TiO_2 (dashed line).

3.2. Calculation of Structural Parameters of the ST Films

The Detailed knowledge of crystallite size and shape in a finely divided powder often helps to correlate many physical properties of a system undergoing transformation in a solid state reaction. The average crystallite size was determined based on XRD peak broadening using the Scherrer equation [24-26].

$$D = \frac{0.9\lambda}{\beta \cos\theta}, \tag{1}$$

where D is average crystallite size, β is the broadening of the diffraction line measured at half maximum intensity (FWHM), λ is wavelength of the x- ray radiation and θ is the Bragg angle.

The specific surface area of ST thick films was calculated using BET method by using the following equation [27]:

$$Sw = \frac{6}{\rho d}, \tag{2}$$

where d is the diameter of the particles, ρ is the density of the particles.

3.3. Microstructure SEM

Fig. 2 depicts the SEM images of (a) pure ST film, (b) CuO-modified ST film (10 min) and (c) most sensitive CuO-modified ST film (20 min). The modified film consists of voids and a wide range of particles with particle sizes ranging from 150 to 250 nm distributed non-uniformly. The CuO-modified film (with dipping time of 20 min) consists of uniform smaller particles associated with larger ones. These particles could be attributed to CuO particles. CuO grains may reside in the intergranular regions of ST. Thus effective surface area was expected to be increased explosively.

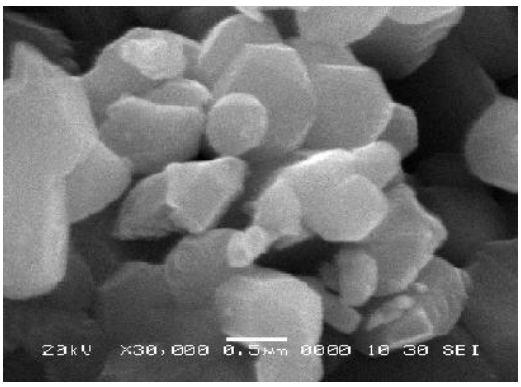

(a)

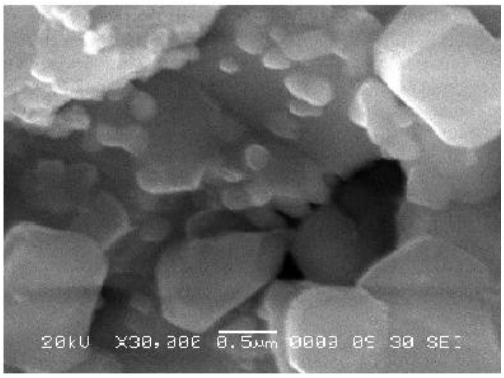

(b)

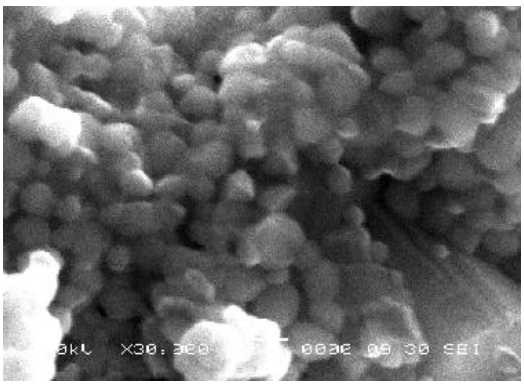

(c)

Fig. 2. SEM images of (a) Pure ST, (b) CuO-modified (10 min), and (c) CuO-modified (20 min).

3.4. Elemental Analysis

The elemental composition, of Sn, Ti, O associated in the sensor element, was carried out using EDS (EOL, JED-2300, Germany) is represented in Table 1. Modified ST films are observed to be more oxygen deficient than the pure ST film. This oxygen deficient would promote the adsorption of relatively large amount of oxygen species favorable for higher gas response. From elemental analysis (Table 1) of ST films, Cuo-modified ST film for 20 min. was observed to be more oxygen deficient.

Table 1. Elemental analysis of unmodified and CuO-modified ST films.

Element (wt %)	Dipping time (min)			
	0	**10**	**20**	**30**
Sn	14.56	18.74	17.06	12.57
Ti	50.07	55.99	58.55	60.57
Cu	0.00	0.19	0.82	1.61
O	35.37	25.08	23.57	25.25

3.5. Structural Parameters and their Analysis

Table 2 shows the crystallite size, particle size and specific surface area of the samples. The grain size is calculated using the Scherrer formula (eq. 1) and XRD data of the calcinated powders. The average particle size was estimated from the SEM images of ST samples and specific surface area from eq.(2). The structural characteristics are summarized in Table 2. One can see that the modified ST film (20 min.) is characterized by the small grain size (24.16 nm) and large active surface area (14.63 m^2/g).

Table 2. Structural characteristics of $Sn_{0.2}Ti_{0.8}O_2$ (ST) thick films.

Sample	**Crystallite(Grain) Size, D nm (XRD)**	**Particle Size, d nm (SEM)**	**Specific Surface Area in m^2/g**
Pure	33.11	500	5.85
Mod (20 min)	24.16	200	14.63

3.6. Thermal Stability of Pure and Cupricated ST Sample

Thermogravimetric analysis (TGA) of samples was carried out using Mettler Toledo Star System - 851 under same condition in static air. The Fig. 3 shows the TGA profiles of pure and cupricated ST films.

It can be concluded from the figure that the cupricated ST was more stable than pure ST. The weight loss in pure is more than cupricated sample for the temperature range 100 ^{0}C to 400 ^{0}C and there was a continuous gain in weight of the cupricated sample after 400 ^{0}C, while the weight of pure sample decreased up to 750 ^{0}C .The increase in weight of the surface cupricated sample (as compared to pure ST sample) can be attributed to the adsorbed oxygen content. The copper oxide on the surface cupricated sample would form misfit regions between the grains of ST and could act as efficient catalysts for oxygenation.

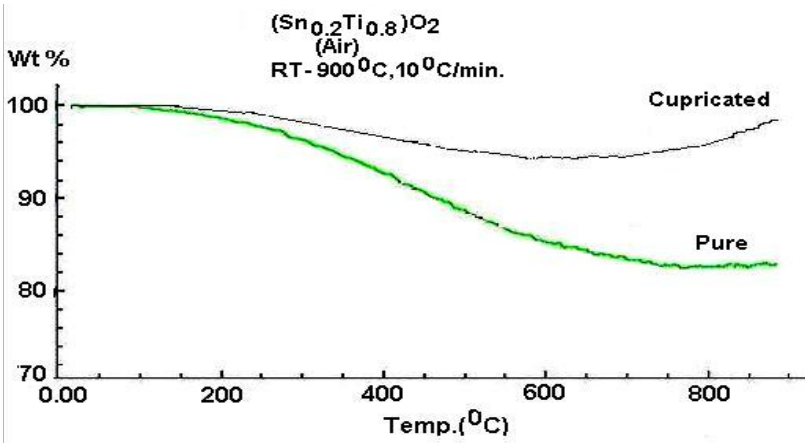

Fig. 3. TGA of pure ST and cupricated ST.

3.7. Thickness Measurement

The thickness of the thick films was measured by using the Taylor-Hobson (Talystep, UK) system. The thicknesses of the films were observed in the range from 75 to 85 μm. The reproducibility of the film thickness was achieved by maintaining the proper rheology and thixotropy of the paste.

3.8. Thermoelectric Power Measurements

Semiconductivity of all ST samples was confirmed by measuring thermolectromotive force of the ST thick film samples. It was observed to be all samples was n-type material.

4. Electrical Properties

4.1. Electrical Conductivity

Fig. 4 represents the variation of conductivity with temperature of ST thick film. The conductivity of these films goes on increasing with increase in temperature, indicating negative temperature coefficient (NTC) of resistance. This shows the semiconducting nature of the films.

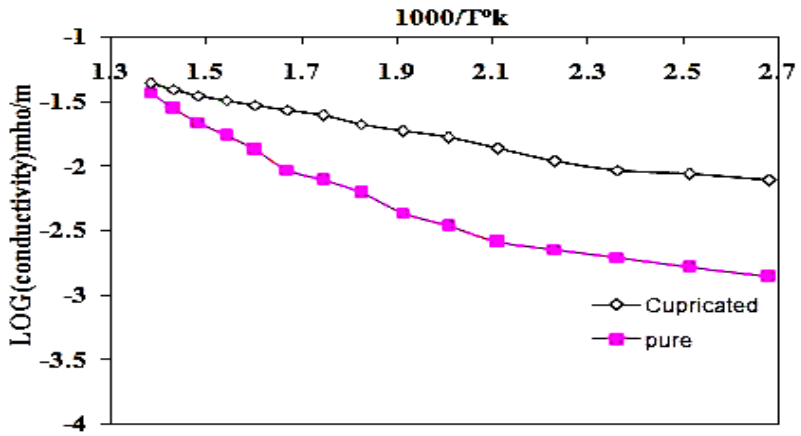

Fig. 4. Variation of Log of conductivity with 1000/ T ^{0}k in air of pure and cupricated ST thick films.

4.2. Electrical Properties

Fig. 5 shows the I-V characteristics of ST thick films for different Sn and Ti molar concentration in air atmosphere. The linearity in the graphs indicates the ohmic nature of the silver contact.

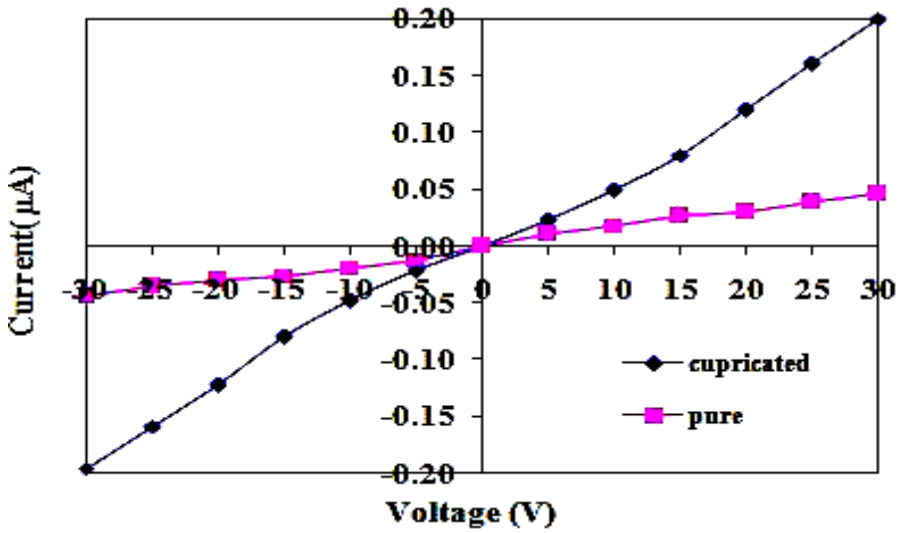

Fig. 5. I-V Characteristics of pure and cupricated ST (x=0.2) thick films.

5. Sensing Performance

5.1. Sensing Characteristics

The response (S) to the gas is defined as:

$$S = \Delta R / R_a = (R_a - R_g) / R_a,$$

where R_a is the ST sensor resistance in air and R_g is the resistance in the test gas at a given temperature [28].

The ability of a sensor to respond to certain gas in the presence of other gases is known as selectivity.

The time taken for the sensor to attain 90 % of the maximum change in resistance on exposure to the test gas is the response time. The time taken by the sensor to get back 90 % of the original resistance is the recovery time.

5.2. Gas Sensing Performance of Pure and CuO-Modified ST Thick Films

Fig. 6 illustrates the sensitivity variation ST sample as a function of operating temperature. Sensitivity measurements were performed at temperatures higher than 100 ^{0}C. At lower temperatures the electrical response to the test gases was low because elevated temperatures are required to change the oxidation state and conductance of ST sample.

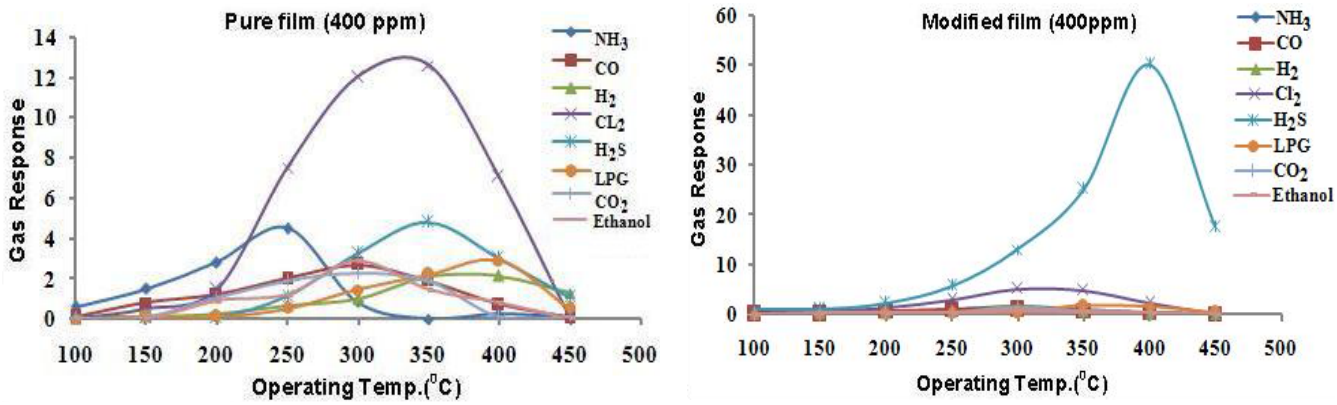

(a) (b)

Fig. 6. Variation of gas response as a function of operating temperature for different gases of (a) pure ST film, and (b) CuO-modified ST film (20 min.)

Some features can be drawn from these figures:

1) Each of the curves shows a maximum of the sensitivity corresponding to an optimum operating temperature of the sensor element. Pure and modified ST films, the sensitivity maximum appears at 350 ^{0}C and 400 ^{0}C respectively. Therefore, the sensors have need of thermal excitation to response to the investigated gases.
2) There are large differences in the sensitivity values to various gases of the pure and modified samples. Pure ST film shows a good response to Cl_2 and CuO- modified ST film shows response to H2S (Fig. 6). Fig. 6 (a) and (b) shows the variation of gas response of pure ST and CuO modified films (fired at 550 ^{0}C) to various gases with operating temperature. The pure ST film shows good response (S=12.6) to Cl2 at 350 ^{0}C for gas concentration 400 ppm and CuO-modified ST film improves the selectivity and sensitivity and maximum response (S=50.2) was found to H2S gas at 400 ^{0}C for same gas concentration. It is clear from the data of elemental analysis that the modified films are observed to be more oxygen deficient and also more specific surface area (14.63 m^2/g) of ST film (dipped 20 min). This oxygen deficient and more surface area would promote the adsorption of relatively large amount of oxygen species favorable for higher gas response.

5.3. Variation of Sensitivity with Dipping Time

Fig. 7 depicts the variation of gas response with dipping time. The film dipped for 20 min showed highest gas response (50.2). The highest gas response could be attributed to the optimum wt% of CuO (0.82 wt %) and its uniform dispersion on the surface of the ST film. The number of oxygen ions adsorbed on this film would have been largest as compared to other CuO-modified films. The larger the number of oxygen ions adsorbed the faster and quicker would be the oxidization of H_2S gas. This would increase the conductance of the film drastically, giving higher response.

5.4. Selectivity of Cupricated ST Film to Various Gases

The ability of a sensor to respond to a certain gas in the presence of other gases is known as selectivity. Fig. 8 shows the bar diagram indicating the selectivity of the pure and cupricated ST films. It is found that the cupricated sensor was highly selective to H_2S gas against NH_3, CO, H_2, Cl_2, LPG, CO_2 and ethanol gases. Selectivity of film would be improved due to surface modification.

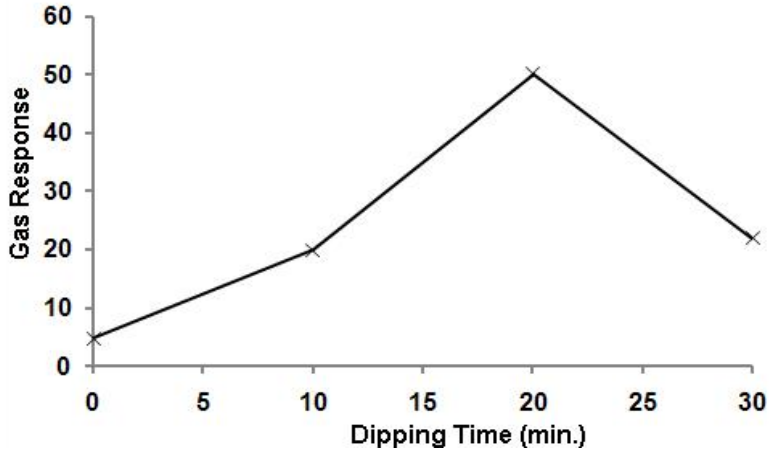

Fig. 7. Variation in gas response to H_2S with dipping time.

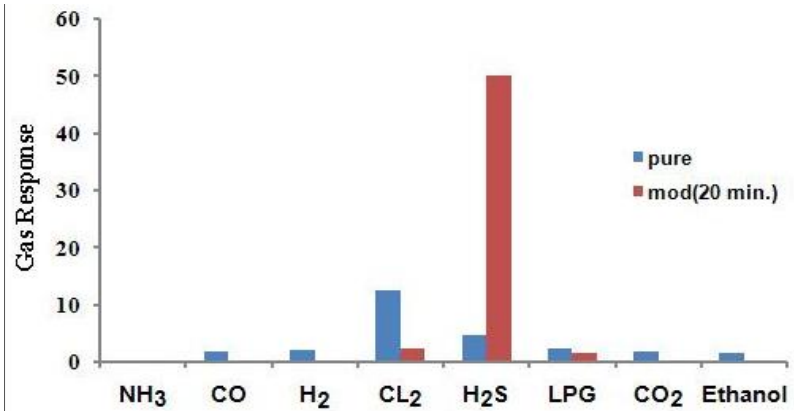

Fig. 8. Selectivity of pure and modified ST film for different gases.

6. Discussion

The gas sensing mechanism belongs to the surface controlled type [20] which is based on the change of the electrical conductance of the semiconducting material upon exposure to different gases. The gas sensitivity is a function of grain size, surface state and oxygen adsorption. The surface cubricateded films can be looked upon as the small particles of copper oxide distributed along the grain boundaries of ST.

The H_2S gas is reducing in nature. On exposure of H_2S gas on the cupricated STfilm, the sensor resistance decreases suddenly giving higher sensitivity. It can reduce CuO into CuS which are metallic in nature and is more conducting. This can be represented as:

$$CuO + H_2S \rightarrow CuS + H_2O \quad (1)$$

Upon subsequent exposure of sensor to air ambient at elevated temperature, sulphides got oxidized and could be recovered back to oxides as

$$2CuS + 4O_2 \rightarrow 2CuO + 2SO_3 \quad (2)$$

When oxygen is adsorbed on the surface of ST, abstracting electrons, and thus an increase in potential barrier at the grain boundaries. When reducing gas such as H_2S is adsorbed between the grains of ST,

the potential barrier decreases as a result of oxidative conversion of the H_2S gas. H_2S reacts with adsorbed oxygen ions as:

$$H_2S + 3O^- \rightarrow H_2O + SO_2 + 3e^- \quad (3)$$

With this reaction, many electrons could release to thick film surface. This could make the Schottky surface barrier decrease; with the depletion layer thinner; consequently, the electrical conductance of the thin film increases. More gas would be adsorbed by the thin film surface; consequently, the gas sensitivity was enhanced. Increase in operating temperature causes oxidation of large number of H_2S molecules, thus producing very large number of electrons. Therefore, conductivity increases to a large extent. This is the reason why the gas sensitivity increases with operating temperature. However, the sensitivity decreases at higher operating temperature, as the oxygen adsorbates are desorbed from the surface of the sensor [29]. Also, at higher temperature, the carrier concentration increases due to intrinsic thermal excitation and the Debye length decreases. This may be one of the reasons for decreased gas sensitivity at higher temperature.

7. Summary and Conclusions

1. The sensing mechanism of the ST was the "surface-controlled gas-sensing mechanism-(adsorption - desorption of oxygen)".
2. $(Sn_xTi_{1-x})O_2$ (ST) for x=0.2 were prepared by wet chemical method.
3. Pure ST film has a good response to Cl_2 gas and CuO-modified ST film has a good response to H_2S gas at optimum working temperature of 350 ^{0}C and 400 ^{0}C respectively.
4. Modified film was selective and sensitive to H_2S can be the film having maximum active surface area and smallest grain size compared to pure film.
5. The pure ST film shows good response (S=12.6) to Cl_2 at 350 ^{0}C for gas concentration 400 ppm and CuO-modified ST film improves the selectivity and sensitivity and maximum response (S=50.2) was found to H_2S gas at 400 ^{0}C for same gas concentration. It is clear from the data of elemental analysis that the modified ST film is observed to be more oxygen deficient, smaller grain size and more specific surface area (14.63 m^2/g). This film could be more selective and sensitive to H_2S.

Acknowledgements

Author (PDH) sincerely thanks to Director, UGC, New Delhi for financial assistance to this research project. The authors thank Management authorities of M.V.P. Samaj, Nasik, The Principal, K.T.H.M. College, Nasik and The Head, Department of Physics, Arts, Commerce & Science College, Nandgaon, Dist: Nasik for providing all the required infrastructural facilities for doing this work.

References

[1]. W. Gopel, K. D. Schierbaum, SnO_2 sensors: current status and future prospects, *Sensors and Actuators, B*, 26-27, 1995, pp. 1–12.

[2]. A. M. Azad, S. A. Akbar, S. G. Mhaisalkar, L. D. Birkefeld, K. S. Goto, Solid-state gas sensors: a review, *J. Electrochem. Soc.,* 122, 1992, pp. 3690–3703.

[3]. J. Zhang, K. Colbow, Surface silver clusters as oxidation catalysts on semiconductor gas sensors, *Sensors and Actuators*, *B*, 40, 1997, pp. 47–52.

[4]. W. K. Choi, S. K. Song, J. S. Cho, Y. S. Yoon, D. Choi, H. -J. Jung, S. K. Koh, H_2 gas-sensing characteristics of SnO*x* sensors fabricated by a reactive ion-assisted deposition with: without an activator layer, *Sensors and Actuators, B*, 40, 1997, pp. 21–27.

[5]. I. Barin, O. Knacke, Thermochemical Properties of Inorganic Substances, *Springer, New York*, 1973, pp. 584–784.
[6]. M. F. Hennaut, P. H. Devigneaud, E. Plumat, Synthesis and properties of conducting materials in the TiO_2–SnO_2 system, *J. Phys. Coll. C1*, 47, 1986, pp. 13–17.
[7]. W. Y. Chung, D. D. Lee, B. K. Sohn, Effects of added TiO_2 on the characteristics of SnO_2-based thick film gas sensors, *Thin Solid Films*, 221, 1992, pp. 304–310.
[8]. N. N. Padurow, Miscibility in the system TiO_2–SnO_2, *Naturwissenschaften*, 43, 1956, pp. 395–396.
[9]. M. Park, T. E. Mitchell, A. H. Heuer, Subsolidus equilibria in the TiO_2–SnO_2 system, *J. Am. Ceram. Soc*., 58, 1975, pp. 43–47.
[10]. M. Batzill, U. Diebold, *Prog. Surf. Sci*., 79, 2005, pp. 47.
[11]. U. Diebold, *Surf. Sci. Rep*., 48, 2003, pp. 53.
[12]. M. Radecka, K. Zakrzewska, M. Rekas, *Sens. Actuators, B*, 47, 1998, pp. 194.
[13]. J. Lin, J. C. Yu, D. Lo, S. K. Lam, *J. Catal.,* 183, 1999, pp. 368.
[14]. V. Dusastre, D. E. Williams, *J. Mater. Chem.,* 9, 1999, pp. 445.
[15]. K. Zakrzewska, M. Radecka, J. Przewoźnik, K. Kowalski, P. Czuba, *Thin Solid Films,* 490, 2005, pp. 101.
[16]. F. R. Sensato, R. Custodio, E. Longo, A. Beltrán, *J. Andrés, Catal. Today*, 85, 2003, pp. 145.
[17]. V. Guidi, M. C. Carotta, M. Ferroni, G. Martinelli, M. Sacerdoti, *J. Phys. Chem., B*, 107, 2003, pp. 120.
[18]. J. D. Lee, Concise In-organic Chemistry, 5th Edition, pp. 698.
[19]. G. S. Manku, In-organic Chemistry, pp. 465.
[20]. G. H. Jain, V. B. Gaikwad, L. A. Patil, Studies on gas sensing performance of $(Ba_{0.8}Sr_{0.2})(Sn_{0.8}Ti_{0.2})O_3$ thick film resistors, *Sens. Actuators, B,* 122, 2007, pp. 605-612.
[21]. C. A. Harper, Hand book of thick film hybrid Microelectronics, *McGraw Hill Book Co.,* New York, 1974.
[22]. G. H Jain, L. A. Patil, M. S. Wagh, D. R. Patil, S. A. Patil, D. P. Amalnerkar, Surface modified $BaTiO_3$ thick film resistors as H_2S Gas sensors, *Sensors and Actuators, B,* 117, 2006, pp. 159-165.
[23]. S. A. Patil, L. A. Patil, D. R. Patil, G. H. Jain, M. S. Wagh, CuO-modified tin titanate thick film resistors as H_2-gas sensors, *Sensors and Actuators B,* 123, 2007, pp. 233-239.
[24]. A. R. West, Solid-state Chemistry and its Application, *Wiley*, New York, 1989.
[25]. A. Klug, I. Alexander, X-ray Diffraction Procedure, *Wiley*, New York, 1962.
[26]. Y. Takahashi, M. Kanamori, A. Kondoh, H. Minoura, Y. Ohya, Jpn. *J. Appl. Phys*. 33, 1994, pp. 6611.
[27]. A. V. Patil, C. G. Dighavkar, S. K. Sonawane, U. P. Shinde, S. J. Patil and R. Y. Borse, Study of Microstructural Parameters of Screen Printed ZnO Thick Film Sensors, *Sensors & Transducers,* Vol. 117, Issue 6, 2010, pp. 62-70.
[28]. N. Rezlescu, E. Rezlescu, F. Tudorache, Gas Sensing Properties of Porous Cu-, Cd- and Zn- Ferrites, *Romanian Reports in Physics*, 61, 2009, pp. 223–234.
[29]. H. Windichamann, P. Mark, *J. Electrochem. Soc*. 126, 1979, pp. 627.
